Cooperative and submolecular dissipation mechanisms of sliding friction in complex organic systems

Daniel B. Knorr, Jr., Tomoko O. Gray, and René M. Overney[a)]
Department of Chemical Engineering, University of Washington, Seattle, Washington 98195, USA

(Received 2 June 2008; accepted 16 July 2008; published online 19 August 2008)

Energy dissipation in single asperity sliding friction was directly linked to submolecular modes of mobility by intrinsic friction analysis, involving time-temperature superposition along with thermodynamic stress and reaction rate models. Thereby, polystyrene served as a representative tribological sample for organic and amorphous complex systems. This study reveals the significance of surface and subsurface (α-, β-, and γ-) relaxational modes, which couple under appropriate external conditions (load, temperature, and rate) with shear induced disturbances, and thus gives rise to material specific frictional dissipation. At low pressures and temperatures below the glass transition point, the phenyl pendant side groups of polystyrene, known for their preferential orientation at the free surface, were noticed to be the primary channel for dissipation of kinetic sliding-energy. While this process was found to be truly enthalpic (activation energy of 8 kcal/mol), energy dissipation was shown to possess both enthalpic and cooperative entropic contributions above the loading capacity of the surface phenyl groups (9.9 kcal/mol) or above the glass transition. Apparent Arrhenius activation energies of frictional dissipation of 22 and 90 kcal/mol, respectively, and cooperative contributions up to 80% were found. As such, this study highlights issues critical to organic lubricant design, i.e., the intrinsic enthalpic activation barriers of mobile linker groups, the evaluation of cooperative mobility phenomena, and critical tribological parameters to access or avoid coupling between shear disturbances and molecular actuators. © *2008 American Institute of Physics*. [DOI: 10.1063/1.2968548]

I. INTRODUCTION

Moving from Amonton's phenomenological description of friction to molecular models, one encounters predominantly generic periodic potentials that are thermally and mechanically inert. From a material perspective, they show little difference from Tomlinson's simple spring model[1] and thus describe energy dissipation in terms of sliding instabilities and phononic excitations, typically occurring when two opposing spring systems temporarily lose contact.[2] While theoretical friction dissipation models[3] and computer simulations[4] have significantly improved in sophistication over the past decade, their applicability is hampered by lack of empirical data, most of which are either of phenomenological nature only, or discuss friction solely at the skin of rigid corrugated surface potentials. The fact that friction indeed also involves intrinsic activation modes (e.g., relaxation modes in organic solid materials) has only been recognized in few isolated studies.[5,6]

This paper provides direct insight into the basic material intrinsic mechanism for frictional dissipation on the submolecular scale of amorphous organic systems. Thereby, two distinct dissipation phenomena are contrasted, namely, the dissipation due to both enthalpic and cooperative processes. Starting from a classical phenomenological description of sliding dissipation involving two distinct friction regimes, a molecular description of the underlying dissipation mechanisms is developed here. A perfectly amorphous tribological model system was chosen in atactic polystyrene (PS), which is known for its multiple relaxation modes and its cooperative relaxation phenomena during the glass forming process.[7] This study illustrates that the entropic (cooperative) contribution to frictional energy dissipation is not only relevant to the polymer melt phase but also to its glass phase. Thereby, two intrinsic modes of dissipation within the glass phase are discussed, as a function of the applied pressure, in terms of activation energies and involvements of cooperative motion. It is shown that the structural properties in the vicinity of the surface can significantly impact the dissipation mechanism.

II. EXPERIMENTAL

Lateral force microscopy (LFM) measurements were performed on an atactic PS film surface (Polymer Source, Inc., M_n=91 000, M_w=96 000, and M_w/M_n=1.05) with a thickness of 280 nm, thick enough to avoid substrate induced confinement effects.[8] The sample preparation involved spin casting a 0.28 wt % solution of PS in toluene onto a silicon surface that has been stripped of its native oxide surface layer by hydrofluoric acid treatment.

Lateral force measurements over a 1 μm scan range were performed at temperatures ranging from 300 to 410 K with a scanning force microscope (SFM) (Topometrix Explorer, Veeco, CA) employing a contact mode lever (PPP-CONT, Nanosensors, nominal and lateral spring constants of ~0.2 N/m and 80 N/m,[9,10] respectively). During the scans, a large line spacing of 20 nm was chosen to limit multiple

[a)]Author to whom correspondence should be addressed. Electronic mail: roverney@u.washington.edu.

scans of the same contact region and thus to avoid scanning induced memory effects. A programmable temperature controller (K-20, MMR Technologies) was used as a temperature control stage. All measurements were performed at ambient pressure under a dry nitrogen atmosphere with relative humidities below 10%.

For this study, uncoated levers were used to avoid any temperature gradient induced stresses in the cantilever beam. Prior to the experiment, cantilever tip apexes were chemical-mechanically etched to smooth the tip surfaces. Thereby, the tips were scanned at low humidities (~10% RH) for 30 min at a 10–50 nN load over silicon wafers with the native oxide layer intact. The silicon wafers were preconditioned by sonication in acetone and methanol for 10 and 40 min, respectively, followed by rinsing with ultrapure 18 MΩ water and vacuum drying for 2 h at 120 °C. The tip etching process results in cantilever tips free of sharp cutting edges. Parallel to the tip etching process, the cantilever torque (lateral spring constant) was determined based on a well established blind-calibration method.[9]

The geometrically preconditioned tips were afterwards passivated and protected by a thin coating of the sample material (PS) that was transferred to the tip during extended scanning (~1 h) at a temperature of increased molecular mobility (generally slightly above T_g, i.e., 100 °C in the case of PS). Passivation of the tip is also required to obtain a well-defined "cohesive" rather than ill-defined "adhesive" contact between the tip and the sample. The contact quality is directly observable from the random moment sampling of the SFM laser beam deflection signal at nonscanning conditions and found to be stabilized for well passivated tips.

The experiments were conducted under isobaric loading conditions by adjusting the normal load (i.e., the sum of the adhesive force and applied load) for each temperature. Thereby, adhesion forces were determined from force-displacement curves at retraction velocities of 1 μm/s. In addition, at each new temperature, the normal and lateral free lever photodiode signals were monitored to determine and correct for instrumental drifts impacting the laser deflection scheme.

III. RESULTS AND DISCUSSION

Figure 1 reveals phenomenological friction-load curves, $F(L)$, obtained by SFM of PS over a range of temperatures and scan velocities. Below T_g, each of the $F(L)$ isotherms reveals a kink at a critical normal load, $L^*(T)$, separating each curve into two linear friction-load branches with friction coefficients $\mu_{\mathrm{I}}(T)$ and $\mu_{\mathrm{II}}(T)$. This phenomenon is apparent with variations in both temperature (Fig. 1) and scan rate (Fig. 1, inset). It is important to note that the absolute values of L^* are dependent on the applied pressure, i.e., involve besides the applied load also the cantilever tip size. The friction force at the critical load, $F^*(L^*(T,v))$, reveals a linear and logarithmic dependence on temperature and velocity, respectively, as expected from thermodynamic friction models.[11,12]

To elucidate the molecular origin for the two friction regimes, we individually collapsed the μ-specific branches

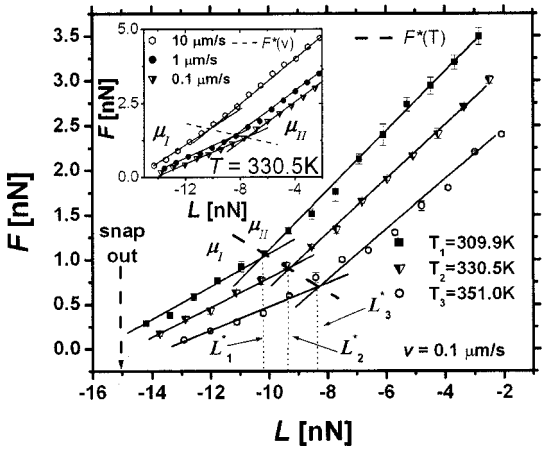

FIG. 1. Isothermal friction-load plots for atactic PS subdivided at critical loads L_k^* $(k=1,2,3)$ into two friction regimes with friction coefficients μ_{I} and μ_{II}. The dashed line tracks critical loads; i.e., $F^*(T)=F_{0,T}-\alpha T$, with $\alpha=8.5$ pN/K and $F_{0,T}=3.7$ nN. (Inset) Friction-load plots at constant temperature with $F^*(v)=F_{0,v}+\beta \ln v$ (dashed line), where $\beta=0.076$ nN and $F_{0,v}=1.5$ nN.

of the isotherms in Fig. 1 into two master curves, by shifting the curves appropriately, i.e., by employing the well known time-temperature superposition principle.[6,13] The results of this process are shown in Figs. 2(a) and 2(b). Two distinctly different apparent activation energies for the two loading regimes μ_{I} and μ_{II} of $E_{a,\mathrm{I}}=8.2\pm1$ kcal/mol (~0.30 eV) and $E_{a,\mathrm{II}}=21.7\pm2$ kcal/mol (~0.94 eV) are revealed in Figs. 2(a) and 2(b), respectively. We refer in the following to this methodology of frictional data treatment as *intrinsic friction analysis* (IFA).

By inspection, $E_{a,\mathrm{I}}$ corresponds to the activation energy E_γ of the γ-relaxation in PS (Refs. 6, 14, and 15) and originates from the hindered rotation of phenyl groups around the C–C bond with the backbone. $E_{a,\mathrm{II}}$ exceeds by about 4 kcal/mol the experimentally[15,16] and theoretically[17,18] determined activation energy E_β of 17–18 kcal/mol for the β-relaxation in PS. Despite this discrepancy, which will be discussed in greater detail below, these results elucidate the increase in the friction coefficient from μ_{I} to μ_{II} by a transition between two distinctly different dissipation mechanisms of molecular origin. Thus, frictional energy dissipation is found to depend on the discrete coupling of the sliding motion with submolecular or molecular actuators, i.e., the phenyl side chain rotation or the backbone translation, respectively.

Considering the disparate number of molecules involved in the two relaxation processes, the question arises as to what degree multiple coupled actuators are involved in the friction dissipation regime μ_{II}, which comprises multiple monomer segments for the translational crankshaft motion. That indeed some cooperativity below the glass transition can be expected has been recently shown with an extended coupling model,[17] in which the β-relaxation (more precisely referred to as the Johari and Goldstein β-relaxation[17,19]) was treated as an intermolecular relaxation process rather than an intramolecular process. These findings are in accordance with a well tested empirical relationship,[19] $E_\beta \sim 24RT_g \approx 18$ kcal/mol for PS with $T_g=100\pm2$ °C.

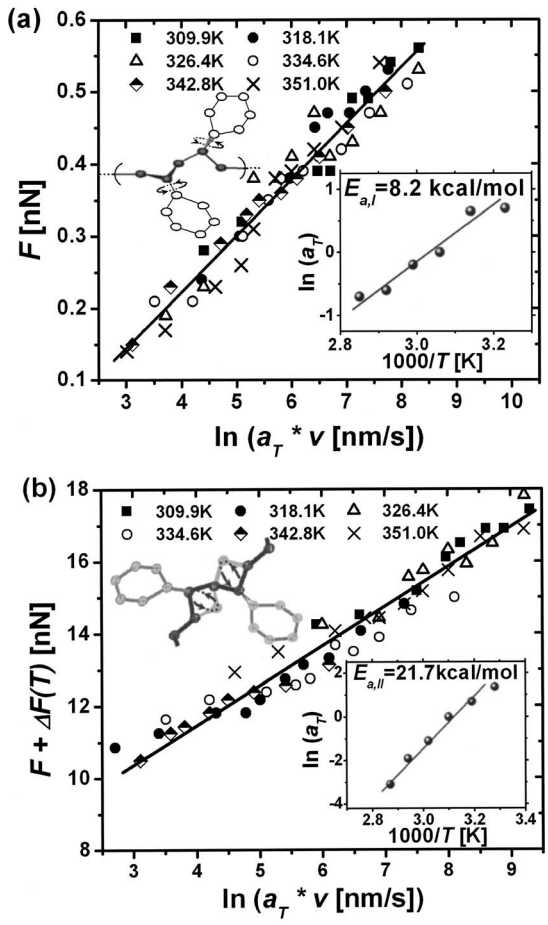

FIG. 2. IFA master curve of glassy PS at an applied load of (a) −14 nN ($< L_1^*|_{T1} = -9.9$ nN). Upper inset: Phenyl group rotation around PS backbone (γ-relaxation). (b) IFA at an applied load of 40 nN above the critical load ($< L_3^*|_{T3} = 7.9$ nN). Upper inset: Local translational backbone motion (β-relaxation). [(a) and (b)] Lower insets: Activation energies of 8.2 and 21.7 kcal/mol from thermal $\ln(a_T)$ vs $(1/T)$ shift factor analysis.

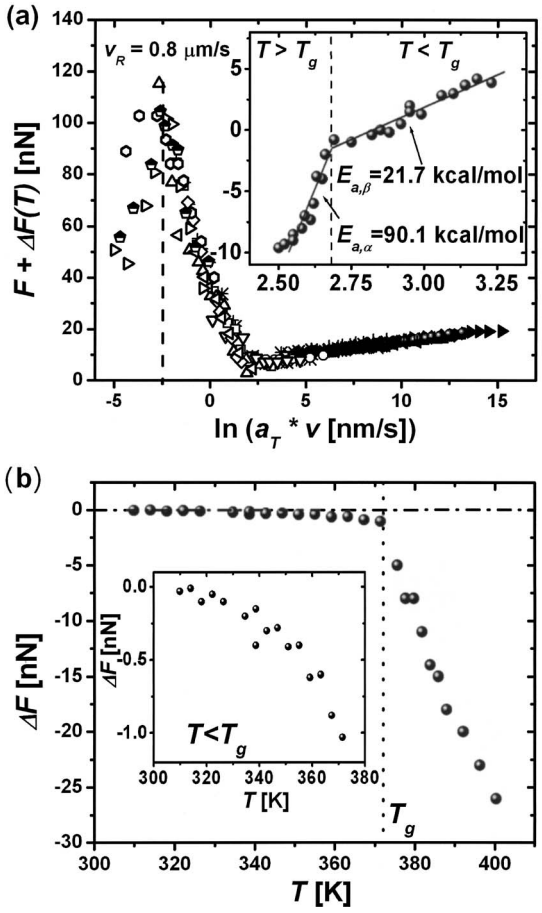

FIG. 3. (a) IFA master curve of PS at 40 nN ($> L_3^*|_{T3} = -7.9$ nN) over a temperature range including T_g. The resonance peak of the α-relaxation is captured. The inset shows activation energies below and above T_g of 21.7 kcal/mol (β-relaxation) and 90.1 kcal/mol (α-relaxation), respectively. (b) Cooperative effect manifests itself by vertical ΔF shifting necessary for collapsing the data to the master curve in (a). Inset: Magnification of ΔF for $T < T_g$.

To evaluate if the above mentioned excess energy of ~4 kcal/mol can be treated as a cooperative entropic contribution, we consider the apparent activation energy E_a, underlying the intrinsic friction dissipation process, to be

$$E_a = \Delta H + RT, \tag{1}$$

with the universal gas constant R. As per Starkweather,[20,21] the frequency, f, of a relaxation is related to the enthalpic contribution ΔH from Eq. (1) as

$$f = \frac{k_B T_R}{2\pi h} d^{-\Delta H/RT} e^{-\Delta S/R}, \tag{2}$$

obtained from the theory of absolute reaction rates, where ΔS, T_R, k_B, and h denote the activation entropy, the relaxation temperature, the Boltzmann constant, and the Planck constant, respectively. Hence, an expression for the apparent process activation energy can be obtained[20,21] as follows:

$$E_a = RT_R[1 + \ln(k_B T_R / 2\pi h f_R)] + T_R \Delta S, \tag{3}$$

where f_R represents the relaxation peak frequency. For a purely activated dissipation process, i.e., a process without cooperativity, the entropic term $T_R\ \Delta S$ vanishes.[20] An example for such a process is the γ-relaxation in PS (friction dissipation regime μ_I), where the side-chain phenyls rotate independently of one another. As we will see below, the degree of coordination can be directly inferred from the vertical shift contribution required to obtain a single master curve.

To determine the degree of cooperativity with Eq. (3), we need information about the relaxation peak, either in terms of a frequency f_R or a velocity v_R, and its corresponding dissipation length ξ.[8] As previously shown,[8] the relaxation peak obtained by dielectric relaxation spectroscopy (DRS) identified by f_R is related to its IFA counterpart v_R via ξ as $f_R = v_R/\xi$. The master curve for PS above T_g in Fig. 3(a) reveals a relaxation peak velocity v_R of 0.8 μm/s. As both IFA and DRS are sensitive to the same relaxation phenomena, relaxation peak frequencies from DRS loss curves can be employed. Thus, DRS frequency data by Wypych *et al.*,[16] i.e., $f_R = 100$ Hz at $T_R = T_\beta = 263$ K, $E_a = 17.0$ kcal/mol yields for the β-relaxation of PS an entropic contribution $T_R \Delta S_\beta$ of 4.5 kcal/mol. This result is in accordance with the excess energy determined above, $E_{a,II} - E_\beta$. Note that the energy component consumed by cooperative motion is significant (>20%) compared to the apparent activation energy.

Repeating this process involving Eq. (3) for the translational motion above T_g (α-relaxation), which has an apparent

activation energy $E_{a,\alpha} \sim 90$ kcal/mol [Fig. 3(a), inset], an entropic contribution of ~70 kcal/mol is deduced. The entropic contribution was determined from $v_R = 0.8\ \mu$m/s at $T_R = T_\alpha = 396.2$ K with the previously determined[8] dissipation length of 0.4 nm. Such a large (~80%) excessive energy contribution to $E_{a,\alpha}$ is expected for the highly cooperative (non-Arrhenius) process of the α-relaxation in polymeric glass formers.[8,22]

The dissipation results for the α- and β-relaxations show that the molecular cooperative energy contribution $T_R\Delta S$ can be a significant contributor to the total frictional energy dissipation. It is important to note that such contributions are omitted by enthalpic models that assume uncoordinated processes only, i.e., involve Gaussian fluctuation-dissipation relations of the form $\langle \xi(t)\xi(t')\rangle \propto k_B T\delta(t-t')$, where $\xi(t)$ represents the random force.

The degree of cooperativity is captured by vertical ΔF force shifting, as illustrated in Fig. 3(b). We find vertical shifting only necessary for processes with nonzero entropic $T_R\Delta S$ components. Truly enthalpic processes (i.e., with $T_R\Delta S = 0$), such as small side-chain relaxations, involve only horizontal shifts. In this special case, E_a is congruent with the "true" activation energy. For processes that are in part cooperative, the intensity (force) shift, ΔF, necessary to collapse the data on a single master curve is indicative of an apparent energy value that exceeds the activation energy.

To illuminate the relationship between the direct experimental observable for cooperativity, ΔF, and the entropic contribution $T_R\Delta S$, we equate the molecular form of Eq. (3), i.e.,

$$E_{\mathrm{ac}} = k_B T_R[1 + \ln(k_B T_R/2\pi h f_R)] + T_R\Delta\bar{S}, \tag{4}$$

where $\Delta\bar{S}$ is $\Delta S/N_A$, $E_{\mathrm{ac}} = E_a/N_A$, where N_A is Avagadro's number, with an expression by Briscoe and Evans[11] for the thermal activation of plastic deformation, i.e.,

$$E'_{\mathrm{ac}} = Q' + P\Omega - \tau\phi, \tag{5}$$

where Q' is the potential barrier height, P is pressure, Ω is the pressure activation volume, τ is the shear stress, and ϕ is the stress activation volume. Setting $\tau/A = (F + \Delta F)$, where A is the true contact area, introducing a term $\phi' = \phi/A$, called the apparent stress activation length,[12] and incorporating the following thermodynamic relationships:[11]

$$F = A\tau_0 + \frac{\Omega}{\phi'}P \quad \text{with } \tau_0 = \frac{1}{\phi}\left(Q' + kT\ln\left(\frac{v}{v_0}\right)\right), \tag{6}$$

where v_0 is a characteristic velocity, we may show (see Appendix) that

$$\Delta F = -\frac{k_B T_R}{\phi'}\left[1 + \ln\left(\frac{k_B T_R \mathrm{v}}{2\pi f \mathrm{v}_0}\right)\right] - \frac{T_R\Delta\bar{S}}{\phi'}. \tag{7}$$

Given that ϕ' is typically on the order of picometers,[12] v_0 is on the order of 20 m/s,[11] and the ratio v/f is on the order of 0.4 nm,[8] the first term on the right hand side of Eq. (7) constitutes only about 5% of the vertical shift for the α-relaxation at $T_\alpha = 396.2$ K, given the above values for $T_R\Delta\bar{S}$, and thus

TABLE I. Entropic summary based on Eq. (23) and Fig. 3.

	α-relaxation	β-relaxation
Temperature (K)	396.2	263.0
$T_R\Delta S$ (kcal/mol)	73.3	4.5
Slope $(\Delta S/\phi')$ (nN/K)	−0.854	−0.0145
ϕ' (nm)	0.0015	0.0085

$$\Delta F \approx -\frac{T_R\Delta\bar{S}}{\phi'}. \tag{8}$$

Comparison of ϕ' to previously reported values[12] is instructive. In order to determine the magnitude of $\phi' = \phi/A$, a contact-area normalized quantity that has physical meaning only in terms of its components (the stress activation volume and the contact area), the previously calculated values of $T_R\Delta S$ were used with the slopes for the α- and β-relaxations obtained in Fig. 3(b) in conjunction with Eq. (8). Table I provides the relevant values for the determination of ϕ' for the two cooperative relaxations, i.e., the α- and β-relaxations. Based on Eq. (8), the slope of $\Delta F(T)$ (as plotted in Fig. 3) is contact-area dependent. For contact radii on the order of 10–100 nm, the stress activation volume $\phi = \phi' A$ ranges from a fraction to hundreds of nm^3, i.e., involving only a few to many molecular segments. Interestingly, the values of ϕ' are on the same order of magnitude as those obtained from liquid lubricated surfaces.[12]

IV. CONCLUSIONS AND OUTLOOK

Closing the loop and returning from the molecular description of the underlying dissipation mechanism in PS to the phenomenological description of frictional dissipation, we found the cause for the discontinuity in the friction-load curve to be a loading dependent activation of two material specific relaxation modes. The known preferential orientation[23] of the phenyl pendant groups toward the free surface normal explains why these two modes are separated by a well-defined transition load. At low load, the phenyls act like surface ball bearings lowering the frictional dissipation significantly. At specific temperature and velocity dependent critical loads, the phenyls are displaced and the "subsurface" or bulk relaxation mode, i.e., the translational crankshaft motion, takes over as the primary dissipation mechanism. This leads to a significant increase in energy dissipation that is caused to a large extent by molecular cooperativity. The transition forces $F^*(v)$ and $F^*(T)$ (see Fig. 1) can also be analyzed in a manner analogous to the IFA energy analysis presented above in accordance with the superposition principle. We deduced from $F^*(v)|_T$-isotherms an activation energy of 9.9 ± 1 kcal/mol, which reflects the phenyl loading capacity at the free surface.

Thus, to grasp the intrinsic subtlety of the underlying molecular dissipation process during single asperity sliding involving a compliant organic system, we had to consider a variety of properties and parameters to fully appreciate the complexity of the process. With the IFA and two thermodynamic models we took into account (i) the structural anisotropy of the material with regard to the free surface, (ii) three

material intrinsic potentials, (iii) external conditions of applied pressure, temperature, and scan velocity, and (iv) the likelihood of molecular cooperativity. Thereby, IFA has proven to be an effective methodology to produce empirical data that are essential for future development of sliding friction models that incorporate more than just thermally and mechanically inert potentials.

ACKNOWLEDGMENTS

This work was supported in part by the University of Washington Initiatives Fund through the Center for Nanotechnology and the Seattle chapter of ARCS, Inc.

APPENDIX: DERIVATION OF EQ. (8)

Both Starkweather[21] and Briscoe and Evans[11] employed an Arrhenius equation to describe either material relaxation phenomena or stress-induced processes. Starkweather considered it to be a viscoelastic relaxation process, wherein the frequency of the relaxation is related to temperature via[20,21]

$$f_R \sim e^{-E_{ac}/k_B T_R}, \tag{9}$$

with the Boltzmann constant k_B and the absolute relaxation peak temperature T_R. This leads to an apparent Arrhenius activation E_{ac} of Eq. (4), repeated here for convenience,

$$E_{ac} = k_B T_R \left[1 + \ln\left(\frac{k_B T_R}{2\pi h f_R} \right) \right] + T_R \Delta \bar{S}, \tag{4'}$$

where f_R, h, and $\Delta \bar{S}$ correspond to the peak relaxation frequency, the Planck constant, and the molecular activation entropy, respectively.

Similarly, Briscoe and Evans[11] described shear as a thermally activated process by employing Eyring's model. Thereby, they assumed plastic deformation in solids to take place by discrete processes involving small numbers of molecules. In the cases of shear stresses (i.e., friction forces) that are proportional to $\ln(v)$, the temperature dependent shear velocity is given as[11]

$$v = v_0 e^{-E'_{ac}/(k_B T_R)} \tag{10}$$

with an apparent Arrhenius activation energy of

$$E'_{ac} = Q' + P\Omega - \tau\phi. \tag{11}$$

Q' is the potential barrier height with respect to the plastic deformation, P is the pressure imposed, Ω is the pressure activation volume, τ is the shear stress, and ϕ is the stress activation volume.

We can proceed by assuming that the apparent Arrhenius activation energies for these two processes are equivalent, i.e.,

$$E'_{ac} = E_{ac}, \tag{12}$$

yielding

$$E'_{ac} = Q' + P\Omega - \tau\phi = k_B T_R \left[1 + \ln\left(\frac{k_B T_R}{2\pi h f_R} \right) \right] + T\Delta \bar{S} = E_{ac}. \tag{13}$$

If we relate the friction force $F+\Delta F$ to the shear stress per unit area τ/A, where F and ΔF represent the measured friction force and the vertical friction shift, respectively, Eq. (13) yields

$$Q' + P\Omega - \phi \frac{(F+\Delta F)}{A} = k_B T_R \left[1 + \ln\left(\frac{k_B T_R}{2\pi h f_R} \right) \right] + T_R \Delta \bar{S}. \tag{14}$$

For convenience, as A cannot be directly obtained in SFM experiments, we define $\phi' = \phi/A$. Thus, ΔF can be expressed as

$$\Delta F = -\frac{k_B T_R}{\phi'} \left[1 + \ln\left(\frac{k_B T_R}{2\pi h f_R} \right) \right] - \frac{T_R \Delta \bar{S}}{\phi'} + \frac{Q'}{\phi'} + \frac{P\Omega}{\phi'} - F. \tag{15}$$

Introducing the stress as

$$\tau = \tau_0 + \alpha P, \tag{16}$$

where $\alpha = \Omega/\phi$,[11] we obtain the following relationships:

$$\tau = \tau_0 + \alpha P = \frac{F}{A} = \tau_0 + \frac{\Omega}{\phi} P, \tag{17a}$$

$$F = A\tau_0 + \frac{\Omega A}{\phi} P = A\tau_0 + \frac{\Omega}{\phi'} P. \tag{17b}$$

Substituting them into Eq. (15) yields

$$\Delta F = -\frac{k_B T_R}{\phi'} \left[1 + \ln\left(\frac{k_B T_R}{2\pi h f_R} \right) \right] - \frac{T_R \Delta \bar{S}}{\phi'} + \frac{Q'}{\phi'} - A\tau_0. \tag{18}$$

The intrinsic stress component τ_0 can be expressed as[11]

$$\tau_0 = \frac{1}{\phi}\left(Q' + k_B T \ln\left(\frac{v}{v_0} \right) \right), \tag{19}$$

where v_0 is a characteristic velocity. Based on this expression the friction force and the friction shift can be expressed as

$$F_F = \frac{A}{\phi}\left(Q' + k_B T \ln\left(\frac{v}{v_0} \right) \right) = \frac{1}{\phi'}\left(Q' + k_B T \ln\left(\frac{v}{v_0} \right) \right), \tag{20a}$$

$$\Delta F = -\frac{k_B T_R}{\phi'} \left[1 + \ln\left(\frac{k_B T_R}{2\pi h f} \right) \right] - \frac{T_R \Delta \bar{S}}{\phi'} - \frac{k_B T_R}{\phi'} \ln\left(\frac{v}{v_0} \right). \tag{20b}$$

To further inspect the vertical frictional shift, we rearrange the current expression of Eq. (20b) to

$$\Delta F = -\frac{k_B T_R}{\phi'} \left[1 + \ln\left(\frac{k_B T_R v}{2\pi h f_R v_0} \right) \right] - \frac{T_R \Delta \bar{S}}{\phi'} = -\frac{k_B T_R}{\phi'} \left[1 + \ln\left(\frac{k_B T_R \xi}{2\pi h v_0} \right) \right] - \frac{T_R \Delta \bar{S}}{\phi'}, \tag{21}$$

in which we introduced the dissipation length ξ (Ref. 8) by substituting f_R with v/ξ. To evaluate the relative importance of the terms in Eq. (21), we evaluated the term to the left above the glass transition by setting $\xi=0.4$ nm at $T_R=396.2$ K,[8] and v_0 within two orders of magnitude around the characteristic velocity of 20 m/s as provided by Briscoe and Evans.[11] It turned out that the term to the right involving $T_R\Delta S=73.3$ kcal/mol dominated the left hand term, which contributed only ~5% to the frictional shift. As such, the argument can be made that for PS, and thus, for many polymer systems,

$$\Delta F \approx -\frac{T_R\Delta\bar{S}}{\phi'}, \tag{8'}$$

i.e., the frictional vertical shift represents a direct measure of the entropic (cooperative) contribution of friction dissipation.

It is important to note that the reference point of vertical shifting for ΔF is arbitrarily chosen, not in a relative sense (relative to the other vertical shifts) but in an absolute sense as long as the same reference temperature is chosen for horizontal shifting. As such, it is conceivable that a constant value can be added to ΔF without loss of generality, i.e.,

$$\Delta F \approx C - \frac{T_R\Delta\bar{S}}{\phi'}. \tag{22}$$

The temperature gradient of $\Delta F(T)$, i.e., $\Delta S/\phi'$, on the other hand, is an absolute quantity of the vertical shift that could be used to obtain ϕ' if $T_R\Delta S$ is known (Table I). It is interesting to note that the lines above and below T_g do naturally intersect, which was not imposed, for instance, by the choice of the reference temperature. As such, the constant, C can be understood as a configurational term at 0 K, dubbed ΔF^0, and thus

$$\Delta F \approx \Delta F^0 - \frac{T_R\Delta\bar{S}}{\phi'}. \tag{23}$$

[1] G. A. Tomlinson, Philos. Mag. **7**, 905 (1929).
[2] R. M. Overney, H. Takano, M. Fujihira, W. Paulus, and H. Ringsdorf, Phys. Rev. Lett. **72**, 3546 (1994); E. Gnecco, R. Bennewitz, T. Gyalog, C. Loppacher, M. Bammerlin, E. Meyer, and H.-J. Güntherodt, *ibid.* **84**, 1172 (2000).
[3] O. K. Dudko, A. E. Filippov, J. Klafter, and M. Urbakh, Chem. Phys. Lett. **352**, 499 (2002).
[4] J. P. Gao, W. D. Luedtke, D. Gourdon, M. Ruths, J. N. Israelachvili, and U. Landman, J. Phys. Chem. B **108**, 3410 (2004); G. T. Gao, R. J. Cannara, R. W. Carpick, and J. A. Harrison, Langmuir **23**, 5394 (2007).
[5] J. A. Greenwood and D. Tabor, Proc. Phys. Soc. **71**, 989 (1958); K. A. Grosch, Proc. R. Soc. London, Ser. A **274**, 21 (1963); K. C. Ludema and D. Tabor, Wear **9**, 329 (1966); K. Vorvolakos and M. K. Chaudhury, Langmuir **19**, 6778 (2003).
[6] S. Sills and R. M. Overney, Phys. Rev. Lett. **91**, 095501 (2003).
[7] S. Sills and R. M. Overney, in *Applied Scanning Probe Methods III*, edited by B. Bhushan and H. Fuchs (Springer-Verlag, Heidelberg, 2006), p. 83.
[8] S. Sills, T. Gray, and R. Overney, J. Chem. Phys. **123**, 134902 (2005).
[9] C. K. Buenviaje, S.-R. Ge, M. H. Rafailovich, and R. M. Overney, Mater. Res. Soc. Symp. Proc. **522**, 187 (1998).
[10] J. H. Wei, M. He, and R. M. Overney, J. Membr. Sci. **279**, 608 (2006).
[11] B. J. Briscoe and D. C. B. Evans, Proc. R. Soc. London, Ser. A **380**, 389 (1982).
[12] M. He, A. Szuchmacher-Blum, G. Overney, and R. M. Overney, Phys. Rev. Lett. **88**, 154302 (2002).
[13] M. L. Williams, R. F. Landel, and J. D. Ferry, J. Am. Chem. Soc. **77**, 3701 (1955).
[14] S. Reich and A. Eisenberg, J. Polym. Sci., Polym. Phys. Ed. **10**, 1397 (1972); P. Hedvig, *Dielectric Spectroscopy of Polymers*, 1st ed. (Wiley, New York, 1977).
[15] H. Gao and J. P. Harmon, Thermochim. Acta **284**, 85 (1996).
[16] A. Wypych, E. Duval, G. Boiteux, J. Ulanski, L. David, G. Seytre, A. Mermet, I. Stevenson, M. Kozanecki, and L. Okrasa, J. Non-Cryst. Solids **351**, 2593 (2005).
[17] K. L. Ngai and S. Capaccioli, Phys. Rev. E **69**, 031501 (2004).
[18] A. Kudlik, S. Benkhof, T. Blochowicz, C. Tschirwitz, and E. Rossler, J. Mol. Struct. **479**, 201 (1999).
[19] G. P. Johari and M. Goldstein, J. Chem. Phys. **53**, 2372 (1970).
[20] H. W. Starkweather, Jr., Macromolecules **14**, 1277 (1981).
[21] H. W. Starkweather, Jr., Macromolecules **21**, 1798 (1988).
[22] E. Donth, J. Non-Cryst. Solids **307–310**, 364 (2002).
[23] S. Akhter, L. Fahlquist, J. M. White, and E. L. Hardegree, Appl. Surf. Sci. **37**, 406 (1989); D. A. Fischer, G. E. Mitchell, A. T. Yeh, and J. L. Gland, *ibid.* **133**, 58 (1998).